Energetic and Thermal Sn Interactions and their Effect on EUVL Source Collector Mirror Lifetime at High Temperatures

J. P. Allain[1,*], M. Nieto[1], M. Hendricks[1], A. Hassanein[1], C. Tarrio[2],
S. Grantham[2], V. Bakshi[3]

[1] Argonne National Laboratory, Argonne, Illinois
[2]National Institute of Standards and Technology, Gaithersburg, Maryland
[3]Sematech, Austin, Texas

ABSTRACT

Exposure of collector mirrors facing the hot, dense pinch plasma in plasma-based EUV light sources remains one of the highest critical issues of source component lifetime and commercial feasibility of EUV lithography technology. Studies at Argonne have focused on understanding the underlying mechanisms that hinder collector mirror performance under Sn exposure and developing methods to mitigate them. Both Sn ion irradiation and thermal evaporation exposes candidate mirrors tested (i.e., Ru, Rh and Pd) in the experimental facility known as IMPACT (Interaction of Materials with charged Particles and Components Testing). Studies have led to an understanding of how Sn *energetic ions* compared to Sn *thermal atoms* affect three main surface properties of the collector mirror: 1) surface chemical state, 2) surface structure and 3) surface morphology. All these properties are crucial in understanding how collector mirrors will respond to Sn-based EUV source operation. This is primarily due to the correlation of how variation in these properties affects the reflectivity of photons in the EUV spectral range of interest (in-band 13.5-nm). This paper discusses the first property and its impact on 13.5-nm reflectivity.

Investigation in the IMPACT experiment has focused on Sn thermal and energetic particle exposure on collector mirrors (Ru, Pd and Rh) and its effect on mirror performance as a function of incident thermal flux, incident ion flux, incident angle and temperature. This is possible by a new state-of-the-art *in-situ* EUV reflectometry system that measures real time relative EUV reflectivity at 15-degree incidence and 13.5-nm during Sn exposure. These results are then compared to at-wavelength EUV reflectivity measurements using the newly upgraded NIST-SURF facility. Sn energetic ions at 1-keV and fluxes of about 10^{13} cm^{-2}s^{-1} are used in conjunction with a moderate flux Sn evaporative source delivering Sn fluences ranging from 10^{15}-10^{17} cm^{-2}. The temperature of the mirror sample is locally varied between 25 and 200 C with the chemical state of the surface simultaneously monitored using X-ray photoelectron spectroscopy, and low-energy ion scattering spectroscopy. Results demonstrate the balance between energetic and thermal Sn has on the total Sn surface fraction during exposure and its effect on the structural and reflective properties of the mirror surface.

Keywords: threshold sputtering, EUV reflectivity, Sn implantation, Sn deposition, EUV collector optics, ion scattering spectroscopy

1. INTRODUCTION

One of the leading factors reducing lifetime and performance of EUV mirrors in EUV lithography sources based on Sn-plasma is contamination by condensed thermal Sn particles and energetic Sn. These contaminants emanate from the pinch plasma in discharge and laser produced plasma sources. The energy distribution of Sn particles varies from thermal to energetic. Thermal particles deposit on the EUV collector mirror surfaces and eventually lead to reduction of 13.5-nm reflectivity by absorption losses and variation of the surface morphology. Energetic particles, charged or neutral, coming from the expansion at the end of the pulse of the high-temperature pinched plasma induces sputtering and moderate surface roughness modification. Off-band radiation couples energy to the mirror in the form of heat where surface mirror temperatures can reach 200-400 C, depending on geometrical mirror design and thermo-mechanical cooling system. Understanding the effect of Sn particles on EUV reflectivity performance is central to determine collector lifetime for Sn-based EUVL sources.

The effect of energetic ions exposed to the mirror material and its effect on EUV reflectivity has been studied in previous work and in this work we cover additional conditions including temperature variation [1-4]. Detailed papers on these issues are also in preparation [4-6]. This work presents some of the most recent results regarding the effect of Sn bombardment and thermal Sn deposition on the reflectivity of single layer mirrors (SLM) at room temperature and with variation of temperature. Material candidates for SLM include Ru, Pd and Rh.

2. EXPERIMENTAL SETUP

2.1 In-situ surface characterization in IMPACT

The Interaction of Materials with Particles and Components Testing (IMPACT) experimental facility has been described in earlier publications and one to be published soon [1,7]. We briefly describe it here and elaborate on the *in-situ* EUV reflectometry system used for some of the results presented in this paper and in previous work. Figure 1 shows a schematic of the at-wavelength EUV reflectometry system configuration. The EUVR system in IMPACT was designed to measure the relative at-wavelength (13.5-nm) reflectivity performance of candidate SLM samples during exposure to either or both thermal and energetic Sn particles. The technique is designed so that all the available surface characterization techniques can be used simultaneously during Sn exposure. This one-of-a-kind system and detailed results is the subject of upcoming publications and only described here in general.

IMPACT is a UHV system where base pressures between 10^{-9} and 10^{-8} Torr are routinely achieved. IMPACT uses several in-situ metrology techniques that are able to measure the local surface atomic concentration of implanted or deposited Sn atoms during either exposure to ions or thermal atoms, respectively. In-situ techniques include low-energy ion scattering spectroscopy (LEISS), Auger electron spectroscopy (AES), X-ray photoelectron spectroscopy (XPS) and extreme ultraviolet photoelectron spectroscopy (EUPS). All these techniques can interrogate the sample during exposure.
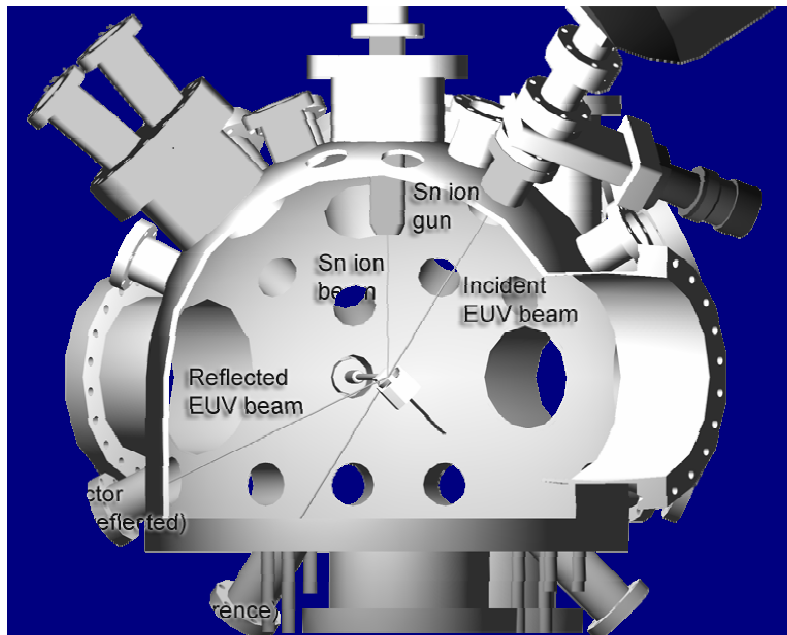

Figure 1: Schematic view of the *in-situ* EUV reflectometry system in IMPACT. A sem|20 EUV Phoenix-EUV tube source of 13.5-nm light is used in total external reflection mode to measure the relative at-wavelength 13.5-nm reflectivity during exposure of mirror samples to either or both thermal and energetic Sn. Filtered EUV photodiodes are used for both thru and reflected configurations.

LEISS gives compositional information about the top monolayer in the sample, while AES and XPS probe the subsurface layers due to 1) probing depth of kinetic electrons in AES and 2) probing depth associated with emitted

photoelectrons' depth range. The techniques complement each other and allow a more reliable identification of components as well as their relative abundance and chemical state. In-situ diagnosis of samples monitors dynamic changes that can occur on a surface during irradiation by an ion beam; for example, radiation-induced segregation may drive certain target components to the surface, while radiation-enhanced diffusion will drive them away from the surface. Such phenomena are usually very hard to study by looking at samples before and after the treatment, since the mere act of transporting them to a different chamber for analysis modifies the surface. In addition, the relative changes of Sn surface atom fraction are inherently connected to exposure dose and thus demanding in-situ diagnosis. Complementing in-situ characterization, absolute 13.5-nm reflectivity is measured *ex-situ* at the NIST-SURF facility.

2.2 In-situ at-wavelength 13.5 reflectometry

An innovative *in-situ* EUV reflectometry system was designed and installed in the IMPACT experiment. This section includes detailed description of the design and implementation of the *in-situ* EUV reflectometer system in IMPACT and its focusing mirror system. The design is such that EUV reflectivity is monitored simultaneously during Sn-ion bombardment or Sn thermal deposition *and* the following in-situ surface characterization: ion scattering spectroscopy, erosion rate measurement, Auger and X-ray photoelectron spectroscopy and EUV photoelectron spectroscopy. This technique allows for the first time a controlled experiment to directly monitor how EUV reflectivity is affected by Sn-ion irradiation under conditions found in EUV source devices while diagnosing the response of the surface. To attain such novel in-situ instrumentation, critical design strategies were implemented including a novel, cost-effective elliptical focusing mirror for EUV light.

The EUV source selected was the sem|20 EUV tube from Phoenix-EUV [8]. The source is based on the same principle used to operate a microfocus x-ray source. A collimated high-energy electron beam impacts on a target, producing photons in the process, as seen in Figure 2. By using a Si target, light at 92 eV (and also at 1.6 keV) is emitted from the target. The source size and location is controlled by focusing and steering the incident electron beam. Source sizes as small as 20 μm can be obtained with the sem|20 tube however, this is primarily limited by the focusing mirror system.
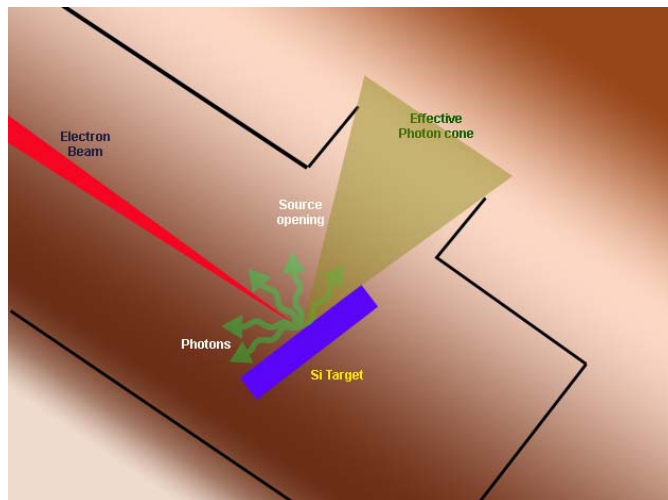

Figure 2: Working principle of the sem|20 EUV source.

Figure 3 presents the angular distribution of photons from the source, with 0° being normal to the Si target inside the source. Due to the location of the source opening, only photons emitted between 64 and 76° from the normal can escape the source enclosure. The question is: what fraction of the total power really leaves the source? A good initial approximation is to integrate between the angles 64 and 75° for θ and the angles -15 and 15° for φ. Then the photon power leaving the source is given by:

$$W = \frac{W_0}{2\pi} \int_{\phi_1}^{\phi_2} d\phi \int_{\theta_1}^{\theta_2} f(\theta) \sin\theta d\theta \qquad (1)$$

Here, $f(\theta)$ is the angular distribution and $W_0/2\pi$ is the total power per steradian. If $f(\theta) = \cos(\theta)$ the integration is trivial and upon evaluating the limits the power coming out of the source is on the order of 1 μW.

The next task of the reflectometer design was sample illumination. This was found necessary since the EUV Phoenix source is an "open" source without any focusing elements. Since the EUV source is a Lambert radiator, the flux of photons drops as the distance from source to sample squared. Assuming a pinhole is used to allow only the solid angle that illuminates the sample, the photon flux is so small that it would be undetectable with the current setup, even at 100% reflection from the mirror sample under study. The solution to this problem is to introduce an optical element that focuses the EUV light from the source onto our sample.
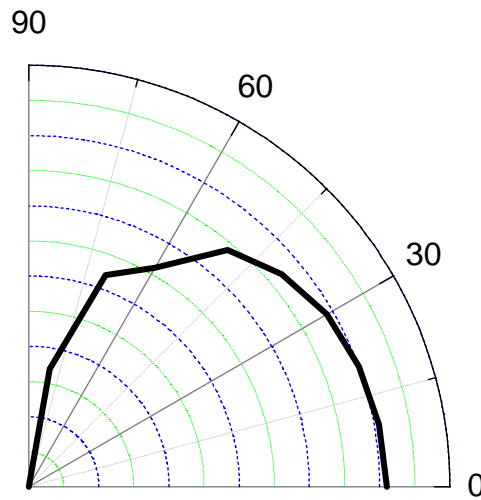

Figure 3: Photon intensity angular distribution for the sem|20 EUV tube.

2.3 Design of the EUV reflectometer optical system

Since the goal is to image one point into another, a natural choice is an elliptical mirror. An elliptical figure mirror has the property of focusing all the rays from a point source into another point, provided the source and the image point are located at the ellipse's foci. The task is to find the parameters of the elliptical shape capable of focusing the light from the EUV source.

Some constrains for the design are already in place due to the chamber design:

- The absolute minimum distance from the mirror center to the sample is 454-mm, which includes the sample-to-flange distance plus a gate valve. This is done using the normal incidence configuration, which requires a longer distance from the source mounting flange to the sample. For the grazing incidence case, the mounting flange has to be extended out 140-mm using an additional CF nipple.
- The mirror can not be mounted inside the IMPACT chamber in order to switch between normal incidence and grazing incidence modes. The mirror is therefore mounted in an auxiliary chamber with an inline vacuum valve.
- The mirror auxiliary chamber needs to be as small as possible, and the mirror insertion into this chamber should be straightforward

- The mirror should be large enough to collect most of the light coming from the source
- The distance from the source to the mirror should be minimized
- An optimal main incident angle should be selected, that balances reflectivity (increased with small angle) and mirror size (increases with mirror size)

The initial step in the design was to fix the distances from the source and the sample to the center of the mirror. These are determined by the distance from the center of the mirror housing chamber (where the mirror will be) to the mounting flanges on said chamber. The only constraint is physical room for these flanges, so as long as the distance allows for placement of flanges the design is set. For this design, the distance from the mirror center to the IMPACT chamber mounting flange was chosen as 76.2 mm, and the distance from the mirror center to the source mounting flange was chosen to be 65.3 mm. This fixes the source to focusing mirror distance at 131.4 mm, and the sample to focusing mirror distance at 530.3 mm.

The next step was to determine the optimal incident angle. This was done by finding a balance between the collected light and the size of the mirror. Here we constrain the mirror size to 6 cm diameter (or any other shape inscribed inside such circle), in order to keep the mirror housing chamber small and be able to fit the mirror into the housing chamber thru a 2.75" ID tube. The geometry of the light cone coming out of the source mounting flange is shown in Figure 4. The light cone is reduced due to the added distance from the source to the mirror chamber opening (35.6-mm). At 0° tilt, the mirror is parallel to the light and there is no collection. For tilt angles greater than 39°, all the light entering the mirror housing chamber is collected.

In addition to geometrical constrains, the EUV reflectivity should be considered as another important factor in determining the optimal incident angle. Figure 5 shows both the light collected and the EUV reflectivity for a Ru mirror with a 6 cm diameter as a function of incident angle. As can be seen from the Figure, the optimal incident angle is close to 26°, when 80% of the light cone is reflected and the reflectivity is about 80%, assuming a perfect Ru mirror. In order to make even the largest expected incident angle small, an angle of 22.5° (half of 45°) was selected, which gives a mean reflectivity of 86% and a collection fraction of 75%.

The ray-tracing program SHADOWVUI was used to calculate the parameters of the mirror. The resultant surface figure is an ellipse with a major axis of 33.1 cm and a minor axis of 10.1 cm. The relevant segment of the ellipse is highlighted in Figure 6. The resultant incident half-angle of the EUV light for IMPACT's EUVR system resulted in 15-degrees with respect to the mirror surface.
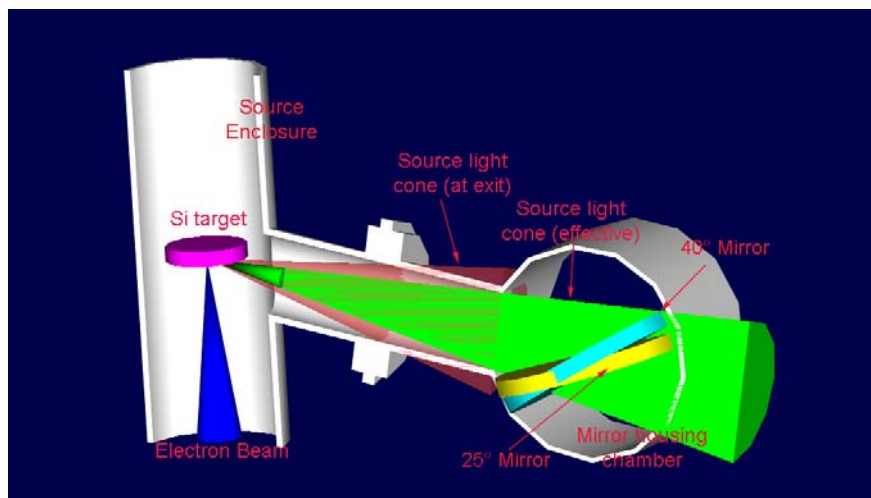

Figure 4: Effective light cone that reaches the mirror from the EUV source (green). The light cone of the source when not attached to the mirror chamber is shown in red.
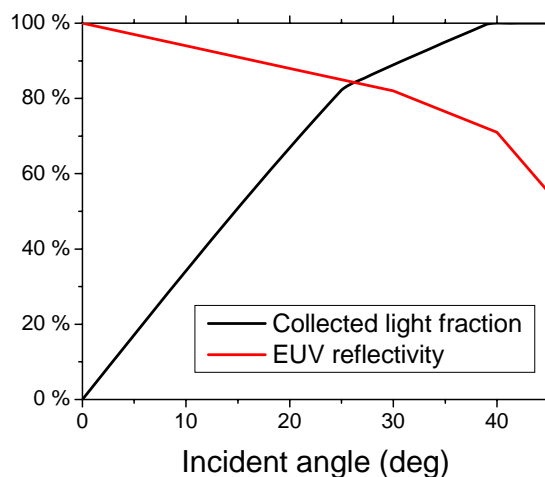
Figure 5: EUV reflectivity and percent of light captured for a 6 cm diameter mirror as a function of mirror tilt.
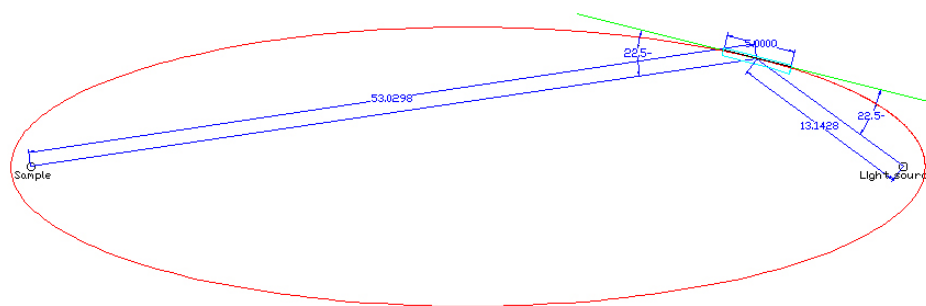

Figure 6: Geometrical rendering of the elliptical section designed for the IMPACT EUV source focusing mirror.

3. RESULTS AND DISCUSSION

Samples in this study were exposed to two kinds of treatment: Sn thermal deposition and Sn implantation. Sn deposition simulates the effect of Sn vapor from the source condensing on the surface of the collector, whereas Sn implantation simulates the exposure of the condenser mirror to energetic Sn ions coming from the hot plasma pinch. Previous work has discussed how this is done in IMPACT [1]. In this work we focused on exposure of a Ru SLM to Sn energetic ions at 1.3-keV. These conditions simulated fast particles in Sn-based EUV sources where off-band radiation induces heating on the mirror.   We also looked at the effect of thermal Sn atoms on a Pd SLM. In particular we examined the effect of surface Sn thermal atom deposition on the EUV 13.5-nm reflectivity. Another study also focused on the Sn atom surface fraction and its variation as a function of temperature. This case also used a Pd mirror material.

Figure 7 shows the result of energetic Sn implanted on a Ru SLM at normal incidence at 1.3-keV.   A key difference between thermal and energetic Sn exposure is the ability of the energetic Sn to remove previously implanted Sn. This results in equilibration of the Sn surface concentration, such that the amount of Sn implanted in the sample equals the amount of Sn leaving the sample as a result of self-sputtering at this energy. This can be clearly seen in Figure 7, which shows the evolution of the Sn atomic fraction on the surface measured in IMPACT with Sn fluence or dose. A dose on the order of 10^{16} ions/cm^{-2} results in saturation of the Sn atomic surface fraction based on LEISS data taken during implantation with 1.3 keV Sn ions and reaches an estimated value of about 50-60%.
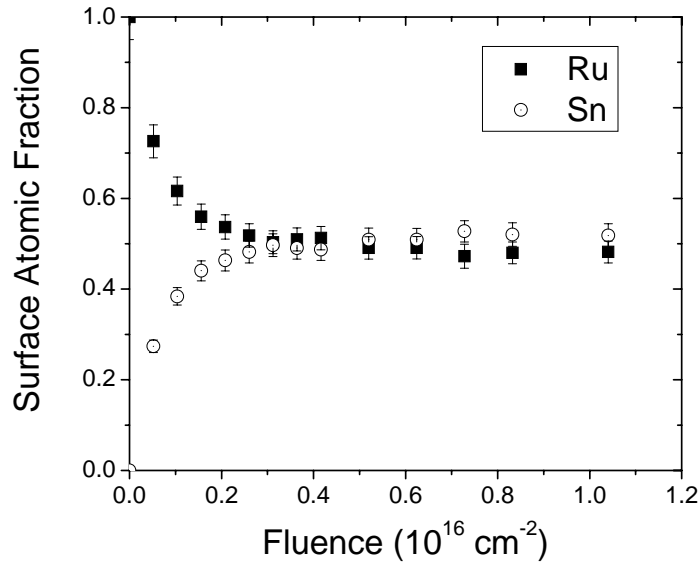
Figure 7: Sn surface atomic fraction during implantation of energetic Sn ions on a Ru SLM at room temperature using low-energy ion scattering spectroscopy.

Figure 8 shows results for the surface Sn fraction measured by LEISS as a function of the Sn fluence also plotted at the equivalent Sn layer thickness. It is described here as "equivalent" due to the fact that Sn does not deposit as smooth single layers during exposure. Instead deposited Sn generates nucleation sites at early stages of deposition and over time agglomerates into islands, which eventually over a large dose equilibrate into nanoscale grains. The details of this growth mechanism are beyond the scope of this paper however Fig. 9 shows the nature of the surface morphology of these mirrors after deposition with Sn. In fact, it is speculated that this partial coverage of Sn on the mirror surface is partially responsible for the LEISS results shown in Fig. 8 where the surface Sn fraction does not reach 100% coverage for the dose exposed. The SEM images in Fig. 9 are for a Ru mirror surface, however the morphology for Pd and Rh surfaces is similar except in the case of Pd, which will be discussed in detail in a future publication.
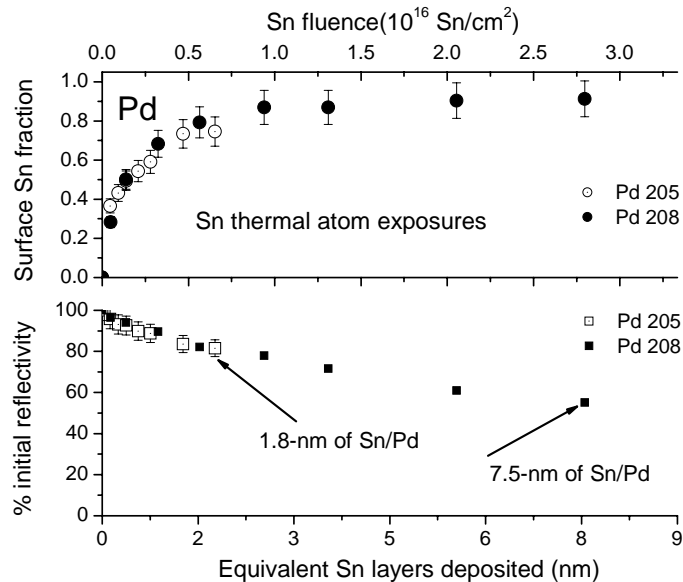

Figure 8: Surface Sn fraction measured by LEISS and relative EUV *in-situ* at-wavelength reflectivity of Pd mirrors exposed to thermal Sn atoms.

(a) 2.5 x 10^{15} cm^{-2}
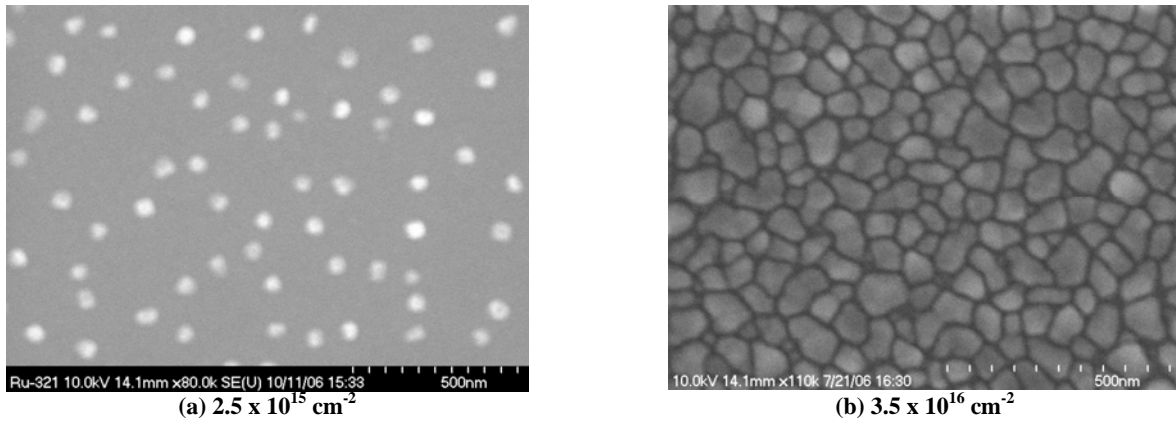

(b) 3.5 x 10^{16} cm^{-2}

Figure 9: Scanning electron micrographs of Rh sample exposed to Sn thermal vapor showing two different exposure doses at room temperature. Similar surface morphology effects are found for Ru mirrors and slightly different for Pd mirrors.

Figure 10 shows the result of a Pd SLM exposed to Sn atoms that reaches an equilibrium surface Sn fraction near 80-85%. The deposition is then followed by a heating cycle that increases the surface mirror temperature to near 225 C and kept there for about 30 minutes. The cycle then continues by cooling the sample down below 100 C. The LEISS data shows the surface Sn fraction as a function of this heating cycle. The result is important in that it demonstrates the sensitivity of surface Sn concentration on the mirror system temperature. First, the data shows evidence that the surface Sn fraction decreases as the temperature is increased. This may be indirect evidence of surface diffusion or diffusion to the mirror bulk. The Pd thin-film mirror is only about 20-nm thin, so there could be some diffusion beyond the Pd mirror material onto the adhesion interface layer and the Si substrate. During the constant heating at 225 C, the Sn surface fraction continues to decrease. This isothermal region is therefore indicative on a stress-induced effect leading to the variation in surface Sn fraction. As the mirror sample is cooled down, the surface Sn concentration does not vary much, therefore suggesting that Sn diffusion into the mirror bulk is likely the explanation for the variation during the heat cycle.
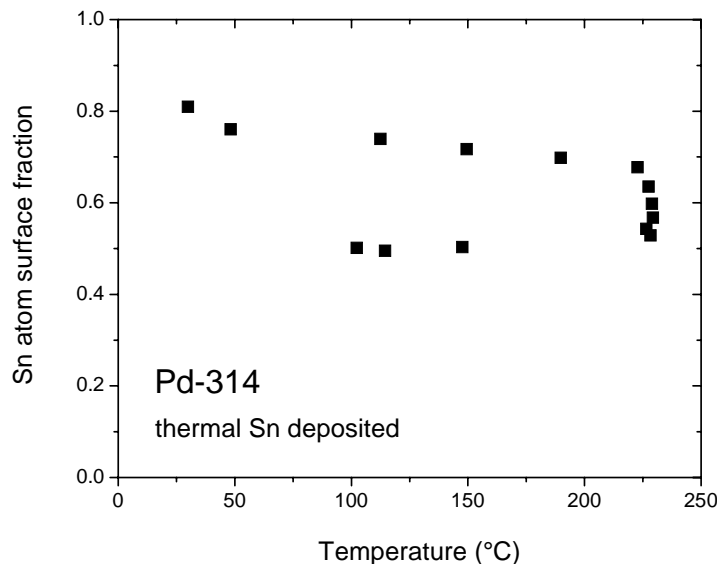

Figure 10: LEISS results of the Sn atom surface fraction as a function of the Pd mirror surface temperature during a heating cycle that reaches 225 C and it's kept at that temperature for about 30 minutes. The cycled then finishes with cooling below 100 C.

The absolute 13.5-nm reflectivity was measured in the NIST-SURF facility for the case of a Pd mirror exposed to thermal Sn at room temperature and at 200 C. These results are shown in Fig. 11. The case for higher temperature seems to suggest that the Pd mirror reflectivity is higher than when Sn is deposited on a cold mirror surface. This could

be indirect evidence that the morphological state of the mirror surface has a direct impact on the EUV reflectivity. Further work will examine how temperature influences the surface kinetics that lead to a particular morphological state (e.g. Sn island growth mechanism) and its correlation to reflectivity response. Suffice to say that here it is clear that temperature has a significant effect on the EUV reflectivity. For example at the incidence of 15-degrees, the relative reflectivity change for the 200 C sample is 10% compared to 25% loss for the R.T. case.
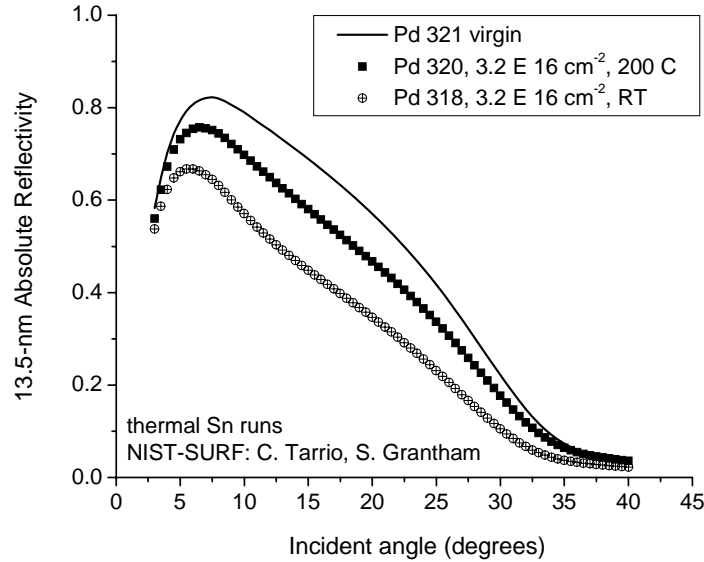

Figure 11: Absolute 13.5-nm reflectivity data taken at the NIST-SURF facility. Pd mirror samples were exposed to 3.2×10^{16} cm^{-2} dose at 200 C and room temperature in IMPACT device. Both results are compared to a virgin sample.

4. CONCLUSIONS

Plasma-facing EUV source device materials will need to be carefully designed to handle the harsh environment they will be exposed to in high-volume manufacturing operation. Collector mirror optics materials have been tested in IMPACT under thermal and energetic Sn particles. We have identified several key properties that are affected by such exposures and that are directly linked to the reflectivity performance of candidate mirrors (Ru, Pd, Rh) at 13.5-nm. In-situ EUV reflectometry data in IMPACT can capture the evolution of the reflectivity during exposure to either energetic or thermal Sn, or both. This capability has opened wide our ability to understand the underlying mechanisms responsible for EUV reflectivity loss during exposure to Sn debris. Further work is necessary to clearly identify the specific mechanisms that link: surface chemical state, structure and morphology to 13.5-nm reflectivity loss.

5. ACKNOWLEDGMENTS

6. REFERENCES

1. J.P. Allain, A. Hassanein, et al., "Effect of charged-particle bombardment on collector mirror reflectivity in EUV lithography devices", Proc. SPIE Int. Soc. Opt. Eng. 6151 (2006) 31.
2. Jean P. Allain, Ahmed Hassanein, Martin Nieto, et al. "Sn-Induced Surface Modification of EUV Plasma-Facing Collector Mirrors", Mater. Res. Soc. Symp. Proc. Vol. 908E (2006) 0908-OO05-27.1
3. J.P. Allain, A. Hassanein, et al., "Erosion and degradation of EUV lithography collector mirrors under particle bombardment", Proc. SPIE Int. Soc. Opt. Eng. 5751 (2005) 1110.

4. M. Nieto, J.P. Allain, A. Hassanein, et al. J. Appl. Phys. 100 (2006) 053510.
5. J.P. Allain, M. Nieto, M.R. Hendricks, A. Hassanein, *"Specular reflectivity of 13.5-nm light from Sn islands deposited on grazing incidence mirror surfaces"* Applied Phys Lett, To be submitted 2007.
6. J.P. Allain, et al., *"Collector mirror performance under Sn ion and atom exposure in EUV plasma-based lithography sources"*, J. Appl. Physics. To be submitted 2007.
7. J.P. Allain, et al., *"Energetic Sn^+ irradiation effects on collector mirror specular reflectivity in the EUV spectral range"*, Applied Phys Lett., To be submitted 2007.
8. André Egbert, Boris Tkachenko, Stefan Becker, Boris N. Chichkov, High Power Laser Ablation V, edited by Claude R. Phipps, Proc. SPIE Vol. 5448, 2004, 693.